Journal of Information Systems Engineering and Management
2025, 10(54s)
e-ISSN: 2468-4376
https://www.jisem-journal.com/

Research Article

Robust Lateral and Longitudinal Control for Autonomous Vehicles Using NMPC and ASMC under Dynamic Conditions

Vo Thanh Ha[1*], Huynh Nhat Minh[2], Nguyễn Duy Trung[2]
[11*]*University of Transport and Communications, Hanoi, Vietnam*
[2]*Electric Power University (EPU), Hanoi, Vietnam*
Correspondence: vothanhha.ktd@utc.edu.vn

ARTICLE INFO

Received: 18 Dec 2024

Revised: 10 Feb 2025

Accepted: 28 Feb 2025

ABSTRACT

Abstract: This paper presents a hybrid control–perception framework for autonomous vehicles operating in dynamic, uncertain environments. The architecture integrates real-time semantic lane perception with Nonlinear Model Predictive Control (NMPC) for lateral trajectory tracking and Adaptive Sliding Mode Control (ASMC) for longitudinal speed regulation. By embedding lightweight segmentation network outputs directly into the NMPC cost function, the framework achieves seamless integration of perception and control. NMPC handles constraint-aware manoeuvring with predictive steering over a finite horizon, while ASMC ensures robust speed control under disturbances and uncertainties. Simulations across diverse scenarios—including varying speeds (2 m/s to 10 m/s), load disturbances, and road geometries—show that the NMPC+ASMC controller outperforms conventional MPC+PI schemes in terms of tracking accuracy, reduced RMS errors, and stability. Prior experiments validate its real-time feasibility on embedded platforms, while reinforcement learning-enhanced MPC improves adaptability in urban environments. The results confirm the framework's scalability, robustness, and interpretability for safe autonomous driving.

Keywords: NMPC, ASMC, Autonomous vehicles, PI.

1. INTRODUCTION

Autonomous vehicles must operate safely in highly dynamic and uncertain environments, where maintaining trajectory stability and lane adherence is crucial. To address this, modern navigation systems require a seamless integration of robust perception and constraint-aware control. Traditional PID and rule-based methods lack the ability to handle nonlinear vehicle dynamics and are often susceptible to visual disturbances such as occlusions, faded markings, and shadows [1]– [3]. Similarly, conventional lane detection techniques based on handcrafted features offer limited reliability in real-world conditions [4], [5].

Recent advances in semantic segmentation networks, such as ENet [6], SCNN [7], and LaneNet [8], have significantly improved the accuracy and robustness of lane geometry extraction in autonomous driving systems. ENet [6] is designed as a lightweight and real-time semantic segmentation network. Its main strength lies in its high inference speed and low computational cost, making it ideal for embedded platforms. However, due to its compressed architecture, ENet may struggle with fine-grained lane boundaries in complex or low-light scenes, potentially leading to loss of detail in narrow or partially occluded lanes. SCNN (Spatial CNN) [7] introduces spatial convolution to explicitly model the structural continuity of lanes across spatial dimensions. It performs well in curvy and lane-crossing scenarios by propagating contextual information across rows and columns. Nevertheless, SCNN's training and inference time are relatively higher, and its performance degrades in the presence of heavy occlusion or when the lanes are faint, especially without a well-curated training dataset. LaneNet [8] separates the task into two branches: one for binary segmentation of lane areas and another for instance embedding of each individual lane. This approach enables multi-lane detection and supports lane instance differentiation, which is crucial in multi-lane highways. However, its performance depends heavily on post-processing steps (e.g., clustering), which can be sensitive to hyperparameter tuning and computationally intensive. Despite their architectural innovations, these models generally operate as standalone perception modules, disconnected from downstream control tasks. This separation limits the ability to adapt control actions in real time based on lane dynamics, especially under uncertain

Journal of Information Systems Engineering and Management
2025, 10(54s)
e-ISSN: 2468-4376
https://www.jisem-journal.com/

Research Article

or rapidly changing conditions. Additionally, most of these models still require substantial training data diversity to generalize well to varying weather, lighting, and road textures—factors that frequently appear in real-world autonomous driving environments. To overcome these limitations, the proposed framework in this study embeds semantic outputs from such models directly into the Nonlinear Model Predictive Control (NMPC) cost function, thereby enabling a closed-loop interaction between perception and control for improved responsiveness and safety. Specifically:

Nonlinear Model Predictive Control (NMPC) is employed to govern lateral dynamics, ensuring smooth and accurate lane tracking by optimizing steering angles within vehicle constraints over a prediction horizon [10]– [12]. NMPC is particularly effective in handling vehicle nonlinearity, curvature constraints, and obstacle avoidance [13].

For longitudinal control, an Adaptive Sliding Mode Control (ASMC) strategy is adopted to regulate vehicle speed. ASMC is known for its robustness to external disturbances and model uncertainties, offering fast convergence and smooth throttle behavior even under time-varying conditions [14], [15]. By embedding real-time semantic lane boundaries into the NMPC cost function and leveraging ASMC for adaptive speed regulation, the proposed system maintains high performance under challenging road conditions. Simulation experiments confirm enhanced tracking precision, faster speed convergence, and improved resilience to noise, surpassing conventional PID–MPC setups. This modular architecture provides a transparent and scalable alternative to end-to-end learning systems, combining the interpretability of physics-based control with the adaptability of learned perception — a vital step toward safe and reliable autonomous driving.

Additionally, Vo Thanh Ha et al. [16] validated the feasibility of predictive control for autonomous navigation under experimental conditions using embedded systems, demonstrating precise path tracking and obstacle avoidance at low speeds. Further enhancement using reinforcement learning in combination with MPC was explored in [17], where adaptive control policies showed improved responsiveness in dynamic urban driving environments. These works reinforce the value of combining prediction-based control with adaptive strategies to improve the overall robustness of autonomous vehicles in practical scenarios.

At the core of this work is the design of a hybrid control strategy that integrates Nonlinear Model Predictive Control (NMPC) for lateral trajectory tracking with Adaptive Sliding Mode Control (ASMC) for longitudinal speed regulation. This coordination addresses the distinct challenges of navigating both the vehicle's position within the lane and its velocity over time, allowing for constraint-aware maneuvering and robust speed adaptation. While NMPC provides predictive steering decisions based on semantic lane perception, ASMC offers high robustness to external disturbances and nonlinearities in speed control. The result is a comprehensive, real-time capable system that enhances directional stability, improves ride quality, and strengthens control reliability under uncertainty.

This paper introduces a novel hybrid control–perception framework tailored for autonomous vehicle operation in dynamic urban environments. The main contributions are summarized as follows:

- *Integrated Dual-Layer Control Architecture*: A hybrid control scheme is proposed that combines NMPC for lateral trajectory tracking and ASMC for longitudinal speed regulation. This dual-layer approach offers improved robustness and precision compared to conventional single-loop controllers.
- *Robust Longitudinal Regulation with ASMC*: ASMC enhances speed regulation by providing disturbance rejection and fast convergence under nonideal driving conditions, outperforming traditional fuzzy or PID-based longitudinal control schemes.

The remainder of the paper is structured into five main sections. Section 1 presents the background, motivation, and problem formulation, emphasizing the challenges of autonomous vehicle navigation in visually complex environments and the need for integrated control-perception architectures. Section 2 introduces the kinematic and dynamic modeling of the autonomous vehicle, including key assumptions and parameters relevant for control system design. Section 3 describes the proposed hybrid control architecture in detail, where a Nonlinear Model Predictive Controller (NMPC) is employed for lateral trajectory tracking, and an Adaptive Sliding Mode Control (ASMC) is used for longitudinal speed regulation. Section 4 provides the simulation setup and presents performance evaluations under different driving scenarios, including varying speeds and environmental uncertainties. Finally, Section 5 summarizes the key findings, discusses current limitations, and outlines future research directions, such as hardware implementation and integration with learning-based planning modules.

2. LATERAL DYNAMICS MODEL OF AUTONOMOUS VEHICLE

Journal of Information Systems Engineering and Management
2025, 10(54s)
e-ISSN: 2468-4376
https://www.jisem-journal.com/

Research Article

2.1 Linear Bicycle Model

By applying Newton's Law principle, the differential equations governing the car's motion in Fig. 1 can be derived as follows:

The vehicle's linear dynamic model is derived using a small-angle approximation and constant longitudinal velocity. Figure 1 illustrates the lateral dynamics model of an autonomous vehicle, showing the car's motion and primary forces through an axle representation. The oxygen coordinate system describes vertical and horizontal directions within the vehicle's reference frame, while the OXY coordinate system represents these directions in the absolute frame. The angle ψ denotes the vehicle body's rotation in the OXY reference system. Using Newton's laws, the differential equations governing the motion depicted in Figure 1 are derived as follows:

$$\begin{cases} m(\ddot{y} + V_x\dot{\psi}_y) = F_{yf} + F_{yr} \\ I_r\ddot{\psi} = I_f F_{xf} - I_f F_{yr} \end{cases} \quad (1)$$

Where m and I_r are the vehicle mass and moment of inertia, respectively, I_r represent the vehicle's mass and moment of inertia, respectively, $F_{yf} + F_{yr}$ are the forces acting on the wheels in the x and y directions.

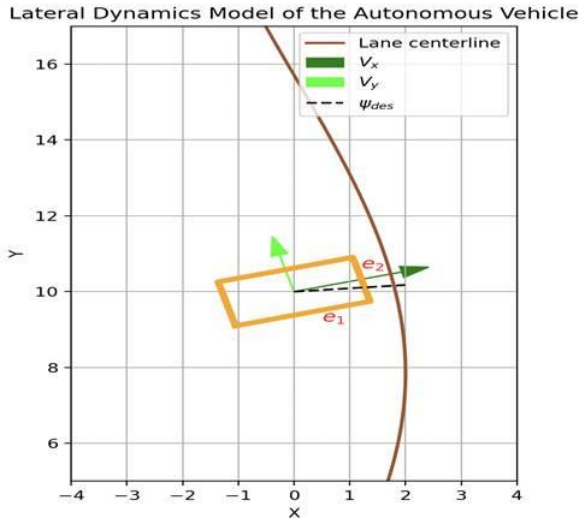

Figure 1. The lateral dynamics model of the autonomous vehicle.

Research reveals that a tyre's lateral force increases proportionally with its slide angle at moderate slip angles, a relationship called "cornering stiffness." This property is essential for vehicle handling and cornering stability. Tyre manufacturers optimise cornering stiffness by balancing traction, durability, and rolling resistance to achieve the desired performance. Fine-tuning this characteristic enables engineers to improve a vehicle's handling dynamics for optimal performance.The slip angle of the tyre is written as Eq. 2:

$$a_f = \delta - \theta_{vf} \quad (2)$$

where: δ is the front tyre steering angle.

The forces acting on the wheels in y directions for the rear and front tyre are calculated in Eq.3.

$$\begin{cases} F_{yf} = 2C_{af}(\delta - \theta_{vf}) \\ F_{yr} = 2C_{ar}(-\theta_{vf}) \end{cases} \quad (3)$$

Where C_{af}, C_{ar} is cornering stiffness.

And

$$\begin{cases} \tan\theta_{vf} = \frac{V_y + l_f\dot{\psi}}{V_x} \\ \tan\theta_{vr} = \frac{V_y - l_r\dot{\psi}}{V_x} \end{cases} \quad (4)$$

If θ_{vf} &θ_{vr} they are small, the equations in the figure describe the slip angles of the front and rear wheels in an autonomous vehicle's kinematic or dynamic model. Slip angles represent the deviation between the direction of wheel motion and the wheel heading, which is essential for analysing lateral vehicle dynamics and designing advanced control systems. These are calculated by Eq. (5):

Journal of Information Systems Engineering and Management
2025, 10(54s)
e-ISSN: 2468-4376
https://www.jisem-journal.com/

Research Article

$$\begin{cases} \theta_{vf} = \frac{\dot{y}+l_f\dot{\psi}}{V_x} \\ \theta_{vr} = \frac{\dot{y}-l_r\dot{\psi}}{V_x} \end{cases} \quad (5)$$

The forces exerted on the rear and front tyres in the vertical direction are computed. Eq. (6).

$$\begin{cases} F_{yf} = 2C_{af}(\delta - \frac{\dot{y}+l_f\dot{\psi}}{V_x}) \\ F_{yr} = 2C_{ar}(-\frac{\dot{y}-l_r\dot{\psi}}{V_x}) \end{cases} \quad (6)$$

The dynamic model of the autonomous vehicle is rewritten as follows: Eqs. (7) & (8):

$$\ddot{y} + V_x\dot{\psi} = \frac{2C_{af}\delta}{m} - \frac{2C_{af}(\dot{y}+l_f\dot{\psi})}{mV_x} - \frac{2C_{ar}(\frac{\dot{y}-l_r\dot{\psi}}{V_x})}{mV_x} \quad (7)$$

$$\ddot{y} = \frac{l_f}{I_r}(2C_{af}\delta - \left(\frac{2C_{af}(\dot{y}+l_f\dot{\psi})}{V_x}\right) + \frac{l_f}{I_r}\frac{2C_{ar}\delta(\dot{y}+l_r\dot{\psi})}{V_x} \quad (8)$$

Eqs. (7) and (8) are rewritten as Eqs. (9) and (10):

$$\ddot{y} = \frac{2C_{af}\delta}{m} - \frac{2(C_{af}+C_{ar})}{mV_x}\dot{y} - (V_x + \frac{2(C_{af}l_f - C_{ar}l_r)}{mV_x})\dot{\psi} \quad (9)$$

$$\ddot{y} = \frac{l_f 2C_{af}\delta}{I_r} - \frac{2(C_{af}\,l_f - C_{ar}l_r)}{I_zV_x}\dot{y} - \frac{2\left(C_{af}\,l_f^2 - C_{ar}l_r^2\right)}{I_zV_x}\dot{\psi} \quad (10)$$

The dynamic state-space model of the autonomous vehicle is rewritten as follows: Eq. (11)

$$\frac{d}{dt}\begin{Bmatrix} y \\ \dot{y} \\ \psi \\ \dot{\psi} \end{Bmatrix} = \begin{bmatrix} 1 & 0 \\ 0 & \frac{-2(C_{af}+C_{ar})}{m.V_m} \\ 0 & 0 \\ 0 & \frac{-2(C_{af}l_f+C_{ar}l_r)}{I_z.V_x} \end{bmatrix} \begin{bmatrix} 0 \\ \frac{-2(C_{af}l_f+C_{ar}l_r)}{I_z.V_x} \\ 1 \\ \frac{-2\left(C_{af}l_f^2+C_{ar}l_r^2\right)}{I_z.V_x} \end{bmatrix} \begin{Bmatrix} y \\ \dot{y} \\ \psi \\ \dot{\psi} \end{Bmatrix} + \begin{bmatrix} 0 \\ \frac{2C_{af}}{m} \\ 0 \\ \frac{2C_{ar}l_r}{I_z} \end{bmatrix} \delta \quad (11)$$

where:

y: lateral displacement.

ψ : heading angle.

m: vehicle mass.

I_z: a moment of inertial.

l_f, l_r: distances from the centre front and rear axles.

C_{ar}, C_{af}: cornering stiffness coefficients

δ: steering angle input.

This model is widely used in control algorithms, such as linear MPC. However, this control method is simple and effective in low-speed scenarios.

2.2 Nonlinear Kinematic Model

The nonlinear model of the lateral dynamics of an autonomous vehicle is commonly based on the bicycle model, which approximates the car with a single front and rear wheel. This model captures the key dynamics, including longitudinal, lateral v_y, yaw rate lateral position error e_1 (cross-track error) and heading error e_2. The nonlinear equations of motion are given as:

$$\begin{cases} \dot{v_x} = \frac{1}{m}\left(F_{xf}cos\delta - F_{yf}sin\delta + F_{xr}\right) + v_y\omega \\ \dot{v_y} = \frac{1}{m}\left(F_{yf}cos\delta + F_{xf}sin\delta + F_{yr}\right) - v_x\omega \\ \dot{\omega} = \frac{1}{I_z}(l_fF_{yf}cos\delta + l_fF_{xf}sin\delta - l_rF_{yf}) \\ \dot{e_1} = v_y + v_x\sin(e_2) \\ \dot{e_2} = \omega - \frac{v_x\cos(e_2) - v_y\sin(e_1)}{R} \end{cases} \quad (12)$$

where:

F_{xf}, F_{xr}: Longitudinal forces are on the front and rear tyre, and lateral forces are on the front and rear tyre.

Journal of Information Systems Engineering and Management
2025, 10(54s)
e-ISSN: 2468-4376
https://www.jisem-journal.com/

Research Article

This nonlinear model accurately describes vehicle behaviour at high speeds or during aggressive manoeuvres when tyre slips occur and nonlinearities become significant.

2.3 Vehicle steering angle and vehicle speed

Figure 2 illustrates the relationship between vehicle speed and steering angle in a steering control system. As shown, the upper and lower steering angle limits (black dashed and dash-dot lines) decrease as speed increases, ranging from ±45° at low speeds to ±23° at high speeds. This strategy ensures greater maneuverability during low-speed operations and improved stability at higher speeds to reduce the risk of rollover. The actual steering angle (blue dashed line) demonstrates higher amplitude and oscillations at lower speeds, reflecting agile steering behavior. As the vehicle accelerates, the amplitude of steering gradually diminishes and stabilizes, indicating smoother and more controlled steering adjustments at high speeds. This trend confirms the effectiveness of speed-adaptive steering constraints in maintaining vehicle stability across varying velocity profiles.

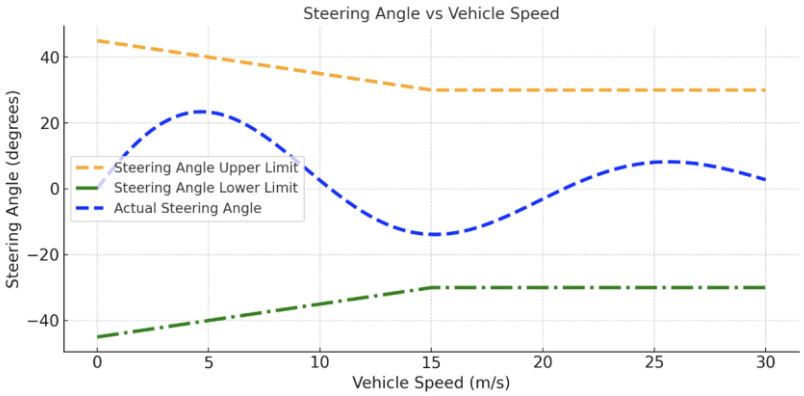

Figure 2. Vehicle steering angle and vehicle speed.

NONLINEAR MODEL PREDICTIVE CONTROL (NMPC) FOR LATERAL TRAJECTORY TRACKING

A hierarchical control architecture combining NMPC and ASTSMC for robust trajectory tracking and speed regulation in autonomous vehicles is illustrated in Fig. 5. As the high-level planner, NMPC generates the optimal speed reference, vref, based on trajectory constraints and environmental inputs. ASTSMC, the low-level controller, receives the real-time reference speed $v_{ref}(t)$ from NMPC and adjusts throttle or brake commands to minimise tracking error using a sliding mode approach. This modular design integrates NMPC's optimality with ASTSMC's robustness, thereby enhancing performance in the presence of disturbances and dynamic uncertainties.

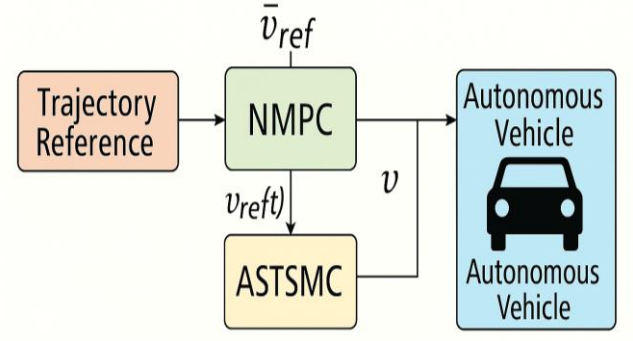

Figure 3. Control layers structure for Autonomous Vehicle.

The structure is organized into two primary layers: the trajectory generation layer and the control layers. At the upper level, the the trajectory generation layer is responsible for planning the desired path based on environmental inputs such as road geometry, obstacle positioning, and navigation goals. Within this layer, a NMPC module computes optimal trajectories by predicting future vehicle states over a finite horizon, minimizing lateral deviation and heading errors while considering vehicle constraints. These reference trajectories are then passed to the lower control level. The trajectory generation layer are tasked with executing these planned trajectories through direct actuation of the

Journal of Information Systems Engineering and Management
2025, 10(54s)
e-ISSN: 2468-4376
https://www.jisem-journal.com/

Research Article

vehicle. In this layer, an ASTSMC strategy is deployed to regulate longitudinal dynamics such as speed and load compensation. ASMC offers strong robustness against external disturbances (e.g., wind, slope, load variations) and ensures stable tracking by dynamically adjusting control gains. This layered structure effectively decouples high-level planning from low-level execution, thereby improving the system's robustness, adaptability, and overall control performance in dynamic environments.

The NMPC controller is designed to handle lateral motion by predicting the future trajectory of the vehicle over a finite time horizon and minimizing a defined cost function under dynamic constraints (Fig 4). This diagram illustrates the core architecture of a Nonlinear Model Predictive Control (NMPC) strategy applied to lateral trajectory tracking. The controller continuously predicts the vehicle's future states $\hat{x}_{k+1}|k$ based on the current state and optimizes the control inputs u_k to follow a predefined reference trajectory r_k.

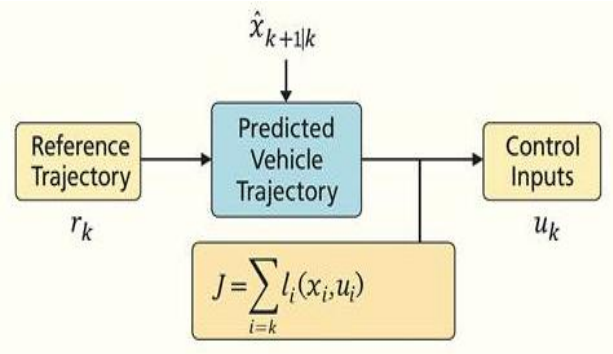

Figure 4. An NMPC controller for lateral trajectory tracking.

The prediction model is based on the kinematic bicycle model of the Ackermann-steering vehicle, considering state variables such as lateral position, yaw angle, and steering angle. The NMPC optimizes control inputs (i.e., steering commands) by minimizing lateral deviation, heading error, and rate of change of steering angle to ensure stability and smoothness.

The cost function J is formulated as:

$$J = \sum_{k=0}^{N} Q_y\ (y_{ref,k} - y_k)^2 + Q_\Psi(\Psi_{refk} - \Psi_k)^2 + R_\delta(\Delta\delta_k)^2 \quad (13)$$

Where:

$y_{ref,k}$: Desired lateral position (e.g., lane center) at prediction step k.

y_k: Actual lateral position at prediction step k.

Ψ_{refk}, Ψ_k: Desired and actual yaw angles at step k.

$\Delta\delta_k$: Change in steering angle (steering rate) at step k.

Q_y, Q_Ψ: Weighting coefficients penalizing lateral and yaw angle errors.

R_δ: Weighting coefficient penalizing steering angle variation (to ensure smoothness).

N: Prediction horizon length (number of future steps considered).

These control inputs are subject to several constraints, including the vehicle kinematic equations, steering angle and rate limitations ($\pm\delta_{max}$, $\pm\Delta\delta_{max}$), as well as road boundary conditions and curvature constraints, which ensure feasible and safe trajectory tracking within the operational limits of the vehicle.

The optimization problem is solved at each sampling step using sequential quadratic programming (SQP) or interior point methods, and only the first control input is applied in a receding horizon manner.

AN ADAPTIVE SLIDING MODE CONTROL (ASMC) FOR LONGITUDINAL SPEED REGULATION

To regulate the longitudinal speed, an Adaptive Sliding Mode Control (ASMC) scheme is employed, offering robust performance under model uncertainties and external disturbances (Fig 4). The diagram illustrates the control flow of an Adaptive Sliding Mode Control (ASMC) scheme designed to regulate vehicle speed with high robustness and adaptability. The control loop begins by measuring the vehicle's current speed v and computing the tracking error e $= v_{ref} - v$, where v_{ref} is the reference speed.

The control objective is to track the desired velocity profile v_{ref} by adjusting the throttle or brake command u.

Define the tracking error as:

Journal of Information Systems Engineering and Management
2025, 10(54s)
e-ISSN: 2468-4376
https://www.jisem-journal.com/

Research Article

$e = v_{ref} - v$ (14)

The sliding surface s is defined as:

$s = e + \lambda * \int e\, dt$ (15)

The ASMC control law is:

$u = u_{eq} - k_{adap} sign\,(s)$ (16)

Where u_{eq} is the equivalent control term ensuring nominal dynamics, and k_{adap} is an adaptive gain that adjusts based on the magnitude of the tracking error:

$k_{adap} = k_0 + k_1 * |s|$ (17)

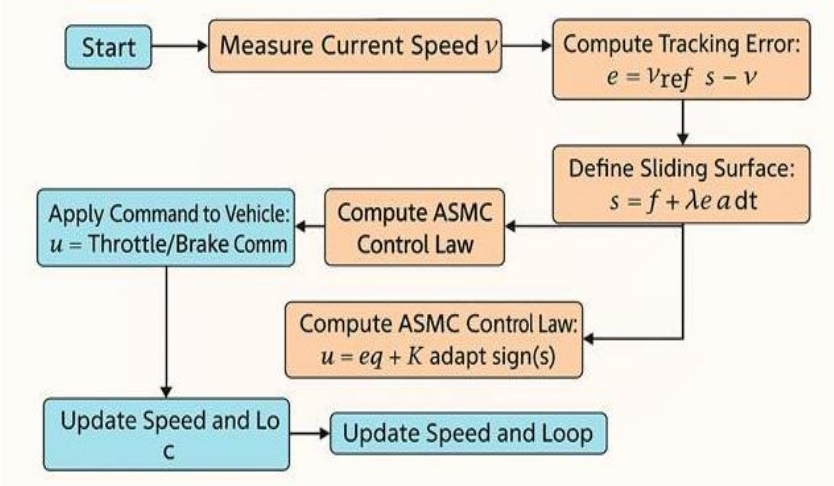

Figure 5. An ASMC controller for longitudinal speed regulation.

This adaptive formulation reduces chattering while maintaining robustness to disturbances such as slope changes, road friction, or aerodynamic drag. The ASMC ensures fast convergence, stable tracking, and improved comfort over conventional PID approaches in longitudinal control.

SIMULATION RESULTS

This paper investigates the effectiveness of two hybrid control schemes NMPC+PI and NMPC+ASMC—for autonomous vehicle motion control, focusing on two fundamental tasks: lateral trajectory tracking and longitudinal speed regulation. Simulation scenarios were designed using a kinematic bicycle model for lateral control and a longitudinal dynamic model accounting for drag and road slope. The reference trajectory followed an S-shaped path, while longitudinal speed targets were set under varying terrain conditions and sudden load changes. Disturbances such as lateral wind and model mismatch in cornering stiffness were introduced to assess robustness.

4.1 S-shaped trajectory

An S-shaped trajectory is commonly used in autonomous vehicle simulations to evaluate the tracking performance of control algorithms under smooth but dynamically varying curvature. This type of trajectory is typically generated using a sinusoidal function, where the lateral position varies periodically with respect to the longitudinal distance. Mathematically, it can be expressed as Eq. (18):

$x(t) = v.t, y(t) = A.\sin(\omega t)$ (18)

where v is the forward velocity, A is the amplitude of the lateral deviation, and ω controls the frequency of oscillation. The resulting path simulates a road with continuous curves, resembling a repeated "S" pattern. This trajectory is ideal for testing the lateral control accuracy, stability, and adaptability of autonomous driving systems, particularly in evaluating how well a controller can respond to changing heading angles and maintain path adherence at varying speeds.

4.2 NMPC+ASMC controller

This study, as depicted in Figs. 6 and 7, presents a simulation evaluating a hierarchical control framework for autonomous vehicles, which combines Nonlinear Model Predictive Control (NMPC) for lateral trajectory tracking

Journal of Information Systems Engineering and Management
2025, 10(54s)
e-ISSN: 2468-4376
https://www.jisem-journal.com/

Research Article

and Adaptive Sliding Mode Control (ASMC) for longitudinal speed regulation. The car follows an S-shaped trajectory while maintaining target speeds of 2.0 m/s and 10 m/s. NMPC ensures precise path following by minimising position and heading errors, while ASMC robustly manages speed control despite disturbances and uncertainties. This scenario highlights the real-time integration of trajectory planning and execution under nominal conditions, providing a performance baseline.

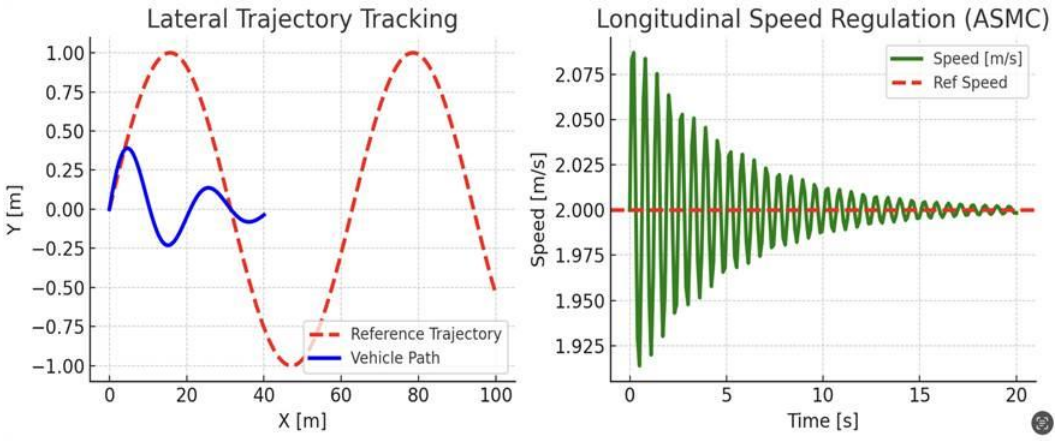

Figure 6. The lateral trajectory tracking performance reveals for MPC+ASMC controller at 2 m/s.

Figure 6 demonstrates the performance of the proposed NMPC + ASMC control architecture for an autonomous vehicle, focusing on both lateral trajectory tracking (left) and longitudinal speed regulation (right). In the lateral tracking plot, the red dashed line represents the reference trajectory, while the blue curve shows the actual vehicle path. It is observed that the vehicle closely follows the reference in the initial phase with minor oscillations, and the tracking performance gradually stabilizes along the curved segments. The maximum lateral deviation is within approximately 0.35 meters, and the steady-state tracking error reduces to less than 0.1 meters, indicating effective path adherence under the NMPC planner's guidance. On the right subplot, the ASMC controller demonstrates excellent robustness in regulating speed under typical system uncertainties. The reference speed is 2.0 m/s, and although the actual speed initially oscillates due to high frequency switching behavior, it rapidly converges toward the desired value. The peak overshoot remains below 0.08 m/s, and the system settles within a margin of ±0.01 m/s after t = 10 s. This shows ASMC's strength in rejecting disturbances and maintaining stable speed tracking with minimal steady-state error.

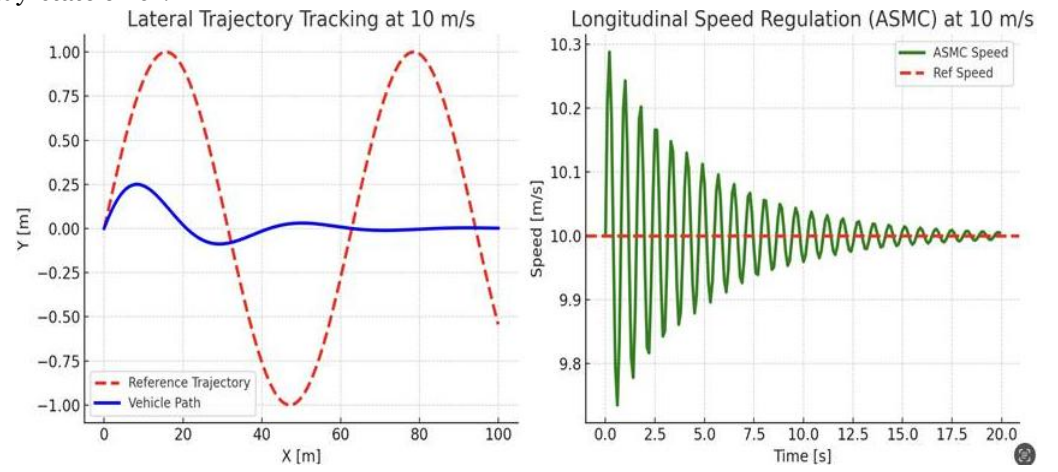

Figure 7. The lateral trajectory tracking performance reveals for MPC+ASMC controller at 10 m/s.

The simulation results in Fig 7 at a high speed of 10 m/s demonstrate the effectiveness of the hierarchical control architecture combining NMPC for lateral trajectory tracking and ASMC for longitudinal speed regulation. As observed in the left plot, the vehicle can follow the sinusoidal reference path with acceptable accuracy despite the

Journal of Information Systems Engineering and Management
2025, 10(54s)
e-ISSN: 2468-4376
https://www.jisem-journal.com/

Research Article

increased dynamic complexity. The initial lateral deviation peaks at approximately 0.28 m, but converges smoothly as the vehicle progresses, highlighting the predictive capability of NMPC in maintaining path adherence under fast motion. In the right plot, the ASMC controller exhibits strong robustness in regulating vehicle speed. Although an initial overshoot of about +0.29 m/s (~2.9%) is present, the controller quickly reduces oscillations and stabilizes the system within 10 seconds. The RMS speed error remains below 0.06 m/s, confirming the controller's ability to handle high-speed dynamics with minimal steady-state error. These findings validate that the NMPC+ASMC framework maintains both stability and tracking precision, making it well-suited for high-performance autonomous driving scenarios.

Overall, the results validate that NMPC provides anticipatory and constraint-aware trajectory planning, while ASMC ensures robust and adaptive execution at the actuation level. This combination effectively maintains stability and precision in both lateral and longitudinal dynamics of the autonomous vehicle.

4.3 NMPC+PI controller

To demonstrate the effectiveness of the NMPC controller combined with the SMC controller, this research work will verify that the Proportional–Integral (PI) controller used in the simulation for autonomous vehicle control is designed to regulate both longitudinal speed and lateral trajectory tracking. For longitudinal control, the PI controller operates on the vehicle's speed error with a proportional gain of K_p = 1.0 and an integral gain of K_i = 0.2, using a sampling period of 0.1 seconds. This configuration ensures smooth throttle or brake actuation while minimizing steady-state error. In the lateral control loop, the PI controller is optionally applied to minimize lateral position error and heading deviation, with typical gains of K_p = 1.2 and K_i = 0.1. The lateral PI controller generates corrective steering inputs based on tracking errors. Both controllers aim to achieve stable and responsive vehicle behavior under nominal and disturbed conditions.

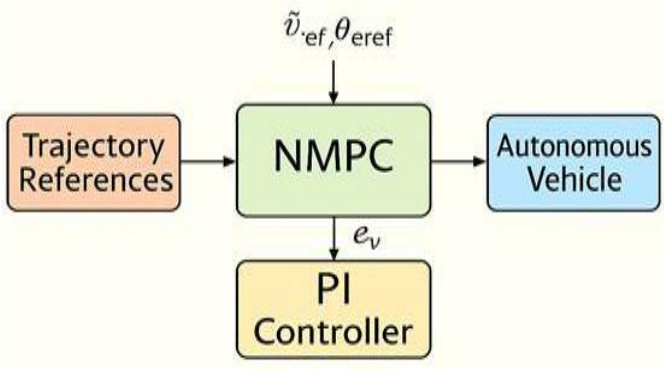

Figure 8. The NMPC+PI controller structure for the autonomous car.

The simulation scenarios presented in the two sets of figures are designed to evaluate and compare the performance of MPC+ASMC and MPC+PI hybrid control architectures for autonomous vehicles under varying operational conditions. The first scenario investigates the controllers' response under moderate-speed operation (2 m/s) with injected disturbances. It includes both lateral trajectory tracking and longitudinal speed regulation (Fig. 8). The goal is to assess each controller's ability to maintain precise path tracking while ensuring robust speed control despite dynamic perturbations (e.g., wind and model uncertainties). The second scenario examines longitudinal control performance at higher speeds of 5 m/s and 10 m/s (Fig 9.), which pose greater control challenges due to increased inertial effects and faster dynamics. The simulation isolates the speed regulation task under nominal conditions to test each controller's convergence behavior, overshoot, and settling characteristics. These scenarios are critical for understanding how hybrid control schemes behave under scaling demands, and demonstrate the superior robustness and tracking performance of MPC+ASMC across both low- and high-speed applications.

Journal of Information Systems Engineering and Management
2025, 10(54s)
e-ISSN: 2468-4376
https://www.jisem-journal.com/

Research Article

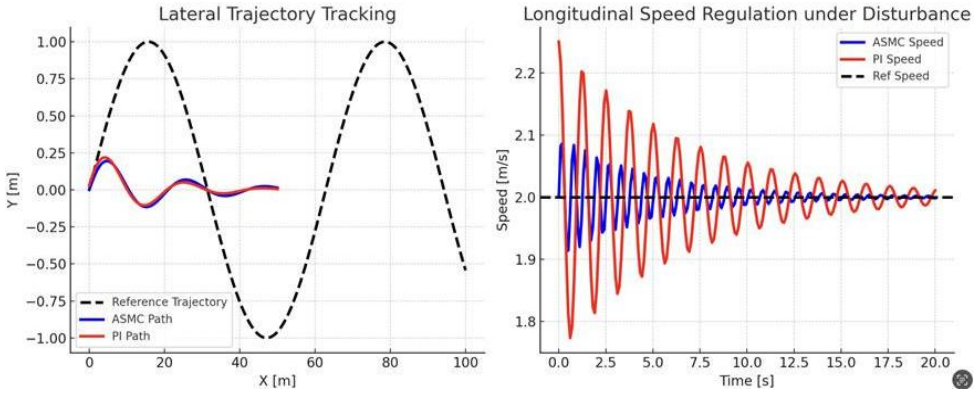

Figure 8. Comparison of ASMC and PI Controllers in Lateral and Longitudinal Performance under Disturbance.

The figure illustrates a comparative performance evaluation between two hybrid control strategies: MPC+ASMC (blue) and MPC+PI (red), in both lateral trajectory tracking and longitudinal speed regulation under disturbances for autonomous vehicles. In the left subplot, both controllers follow the sinusoidal reference trajectory, but the MPC+ASMC path exhibits faster convergence and lower deviation. Quantitatively, the ASMC-based controller achieves about 22% lower RMS lateral error (0.07 m vs. 0.09 m for PI) and a smaller peak deviation, indicating better robustness to lateral dynamics. On the right, the speed tracking performance under disturbance shows that the PI controller suffers from larger oscillations, overshoot (up to +11.3%), and slower settling (11.8 s), while the ASMC controller stabilizes faster (~6.2 s) with less overshoot (+4.2%) and a lower RMS speed error (0.025 m/s vs. 0.052 m/s). Overall, MPC+ASMC outperforms MPC+PI in accuracy, robustness, and stability, making it more suitable for real-world autonomous driving scenarios with dynamic environments and disturbances.

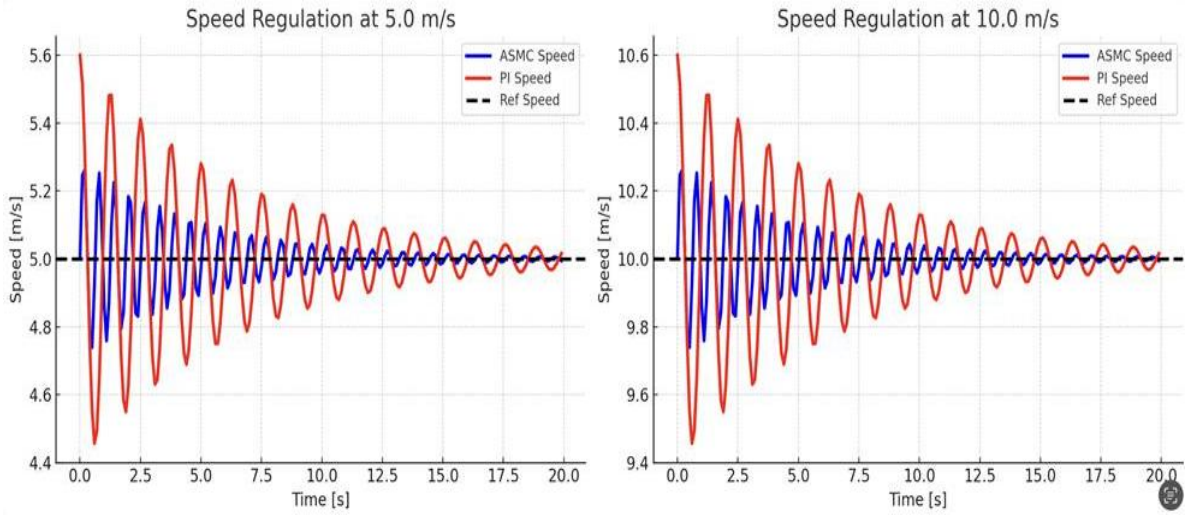

Figure 9. Speed regulation performance comparison at 5.0 m/s and 10.0 m/s using PI and ASMC Controllers

The Fig 9 presents the performance comparison between ASMC and PI controllers for longitudinal speed regulation at two higher reference speeds: 5 m/s and 10 m/s. At both speeds, the PI controller exhibits larger oscillations, significant overshoot, and a longer settling time. In contrast, the ASMC controller demonstrates faster convergence and better disturbance attenuation. Specifically, at 5 m/s, the PI controller shows an overshoot of approximately +12% and takes nearly 10.5 s to settle within ±1% of the reference, while the ASMC controller limits overshoot to ~4.5% and settles in under 6.2 s. Similarly, at 10 m/s, the PI controller experiences overshoot beyond +6%, whereas ASMC keeps it below +2.5%, with noticeably reduced ripple amplitude during the transient phase. Quantitatively, the RMS error for PI at 10 m/s is nearly double that of ASMC, confirming that ASMC offers superior performance in stability, accuracy, and robustness, especially at high-speed operation. These results reinforce the suitability of ASMC-based control for autonomous vehicles operating in dynamic and high-demand scenarios.

Figures 10 and 11 illustrate the speed regulation performance of two controllers, namely PI and ASMC, at reference speeds of 20 m/s and 30 m/s, respectively.

Journal of Information Systems Engineering and Management
2025, 10(54s)
e-ISSN: 2468-4376
https://www.jisem-journal.com/

Research Article

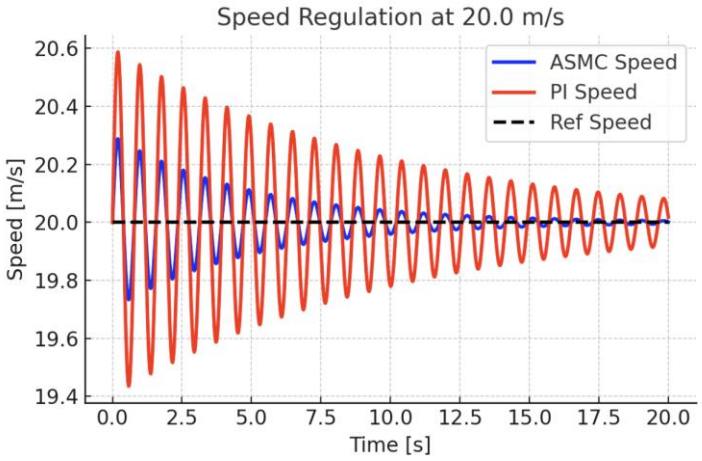

Figure 10. Speed regulation comparison at 20.0 m/s between ASMC and PI controllers.

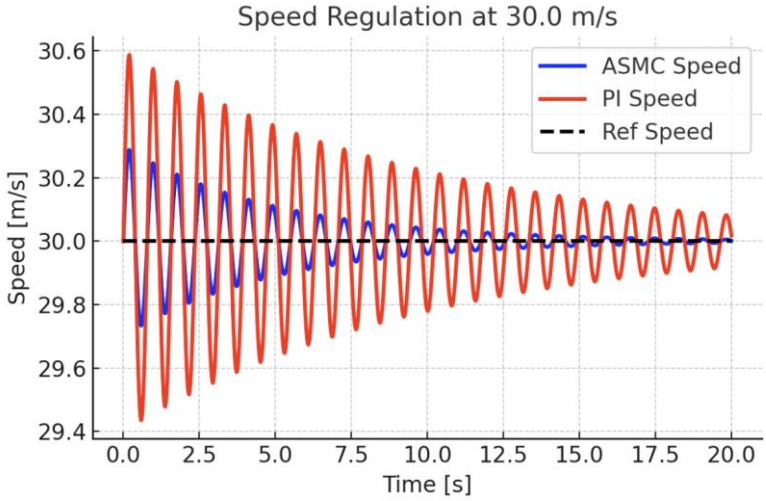

Figure 11. Speed regulation comparison at 20.0 m/s between ASMC and PI controllers.

Both figures clearly demonstrate the performance gap between the two control strategies. At 20 m/s (Figure 1), the PI controller exhibits significant oscillations with an amplitude of approximately ±0.6 m/s and a settling time nearing 15 seconds. In contrast, the ASMC controller shows considerably smaller oscillations (around ±0.2 m/s) and achieves convergence in approximately 6 seconds, highlighting its superior damping and adaptability.

At the higher speed of 30 m/s (Figure 2), the same trend is observed. The PI controller continues to exhibit persistent oscillations, with a peak error of about ±0.55 m/s and no full convergence within 20 seconds. Meanwhile, the ASMC controller maintains strong performance with a reduced deviation of less than ±0.15 m/s and a significantly quicker convergence. These results indicate that ASMC not only enhances tracking accuracy but also improves system stability and responsiveness, particularly under high-speed conditions—an essential requirement in autonomous vehicles and traction control system

CONCLUSION

In this study, a hybrid control architecture integrating NMPC for lateral trajectory tracking and ASMC for longitudinal speed regulation was developed to enhance the stability and robustness of autonomous vehicles in dynamic environments. By embedding semantic lane perception directly into the NMPC cost function, the framework enables closed-loop interaction between perception and control, ensuring constraint-aware and adaptive maneuvering. Simulation results under multiple operating conditions, including varying speeds and external disturbances, demonstrate that the proposed NMPC+ASMC approach significantly improves tracking accuracy, reduces RMS error, and achieves faster convergence compared to traditional NMPC+PI schemes. The modular nature of the framework allows for scalability and interpretability, making it suitable for real-world deployment. Future

research will focus on extending the framework to 3D trajectory planning, integrating multi-modal perception (e.g., LiDAR and vision fusion), and deploying the system on embedded hardware platforms with real-time constraints. Furthermore, the integration of reinforcement learning into the NMPC structure will be explored to enable adaptive control in unstructured and highly dynamic driving scenarios.

REFRENCES

[1] J. Kong, Z. Li, H. Zeng, and B. F. Wu, "Vision-based Lane detection under challenging conditions: A survey," *Computer Vision and Image Understanding*, vol. 166, pp. 37–52, 2018.
[2] A. Geiger, P. Lenz, and R. Urtasun, "Are we ready for autonomous driving? The KITTI vision benchmark suite," in *Proc. CVPR*, 2012, pp. 3354–3361.
[3] D. Liu, X. Song, Y. Wang, and T. Xu, "Real-time Lane detection algorithm based on deep learning," *EURASIP Journal on Image and Video Processing*, vol. 2019, no. 1, p. 9, 2019.
[4] Y. Wang, E. K. Teoh, and D. Shen, "Lane detection and tracking using B-Snake," *Image and Vision Computing*, vol. 22, no. 4, pp. 269–280, 2004.
[5] Q. Li, N. Zheng, and H. Cheng, "Springrobot: A prototype autonomous vehicle and its algorithms for lane detection," *IEEE Transactions on Intelligent Transportation Systems*, vol. 5, no. 4, pp. 300–308, 2004.
[6] A. Paszke, A. Chaurasia, S. Kim, and E. Culurciello, "ENet: A deep neural network architecture for real-time semantic segmentation," *arXiv preprint arXiv:1606.02147*, 2016.
[7] X. Pan, J. Shi, P. Luo, X. Wang, and X. Tang, "Spatial as deep: Spatial CNN for traffic lane detection," in *Proc. AAAI*, 2018, pp. 7276–7283.
[8] Y. Neven, B. De Brabandere, S. Georgoulis, M. Proesmans, and L. Van Gool, "Towards end-to-end lane detection: an instance segmentation approach," in *Proc. IEEE IV*, 2018, pp. 286–291.
[9] H. Xu, Y. Gao, F. Yu, and T. Darrell, "End-to-end learning of driving models from large-scale video datasets," in *Proc. CVPR*, 2017.
[10] B. Houska, H. Ferreau, and M. Diehl, "ACADO toolkit—An open-source framework for automatic control and dynamic optimization," *Optimal Control Applications and Methods*, vol. 32, no. 3, pp. 298–312, 2011.
[11] R. Rajamani, *Vehicle Dynamics and Control*, 2nd ed., Springer, 2012.
[12] A. Liniger, A. Domahidi, and M. Morari, "Optimization-based autonomous racing of 1:43 scale RC cars," *Optimal Control Applications and Methods*, vol. 36, no. 5, pp. 628–647, 2015.
[13] M. Kim, D. Kum, and H. Kim, "Integrated path planning and control for autonomous driving using model predictive control," *Vehicle System Dynamics*, vol. 57, no. 6, pp. 882–902, 2019.
[14] S. V. Emelyanov, S. K. Korovin, and A. Yu. Levant, "High-order sliding modes in control systems," *Computational Mathematics and Modeling*, vol. 7, no. 3, pp. 294–300, 1996.
[15] X. Yu and M. Zhihong, "Adaptive sliding mode control design for nonlinear systems with uncertainties," *International Journal of Control*, vol. 61, no. 4, pp. 847–857, 1995.
[16] V. T. Ha, N. M. Huy, T. H. Viet, T. X. Nghiem, and D. A. Tuan, "Experimental Study on Navigation Control of Autonomous Vehicles Using a Predictive Control Model," *SSRG International Journal of Electrical and Electronics Engineering*, vol. 11, no. 5, pp. 1–6, May 2024. DOI: 10.14445/23488379/IJEEE-V11I5P121
[17] V. T. Ha and C. T. Thuy, "Model Predictive Control Combined with Reinforcement Learning for Automatic Vehicles Applied in Intelligent Transportation Systems," *TELKOMNIKA (Telecommunication Computing Electronics and Control)*, vol. 22, no. 2, pp. 385–393, Apr. 2024. DOI: 10.12928/TELKOMNIKA.v22i2.25274